

ESC-TR-2006-090

**Technical Report  
1123**

# **Extended Radar Return from a Rocket Engine: A Thermal Model**

M.L. Burrows

18 December 2008

---

**Lincoln Laboratory**  
MASSACHUSETTS INSTITUTE OF TECHNOLOGY  
*LEXINGTON, MASSACHUSETTS*



Prepared for the Missile Defense Agency under Air Force Contract FA8721-05 C-0002.

Approved for public release; distribution is unlimited.

**20090112239**

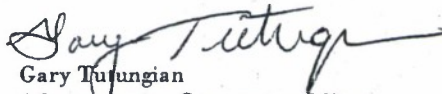
This report is based on studies performed at Lincoln Laboratory, a center for research operated by Massachusetts Institute of Technology. This work was sponsored by the Missile Defense Agency under Air Force Contract FA8721-05-C-0002.

This report may be reproduced to satisfy needs of U.S. Government agencies.

The ESC Public Affairs Office has reviewed this report, and it is releasable to the National Technical Information Service, where it will be available to the general public, including foreign nationals.

This technical report has been reviewed and is approved for publication.

FOR THE COMMANDER



Gary Tutungian  
Administrative Contracting Officer  
Acquisition Enterprise Division

Non-Lincoln Recipients

PLEASE DO NOT RETURN

Permission has been given to destroy this document when it is no longer needed.

**Massachusetts Institute of Technology  
Lincoln Laboratory**

**Extended Radar Return from a Rocket Engine: A Thermal Model**

*M.L. Burrows  
Group 34*

**Technical Report 1123**

**18 December 2008**

**Approved for public release; distribution is unlimited.**

**Lexington**

**Massachusetts**

**This page intentionally left blank.**

## ABSTRACT

Cavities generate delayed radar returns. But because the standard scattering models are overwhelmed by the complexity of the problem, no predictive physical model of cavity scattering has been available to describe what is observed.

The delayed return is caused by the slow disgorgement of the radar energy captured by the cavity. For some cavities, and especially for the liquid-fueled rocket engine, the length of the extended return is many times the maximum dimension of the cavity. Since this implies that the radar energy undergoes a great many internal reflections before it reemerges, it suggests treating the captured energy within the cavity as a well-mixed thermal radiation field.

This suggestion leads to a simple scattering model for the well-mixed lossless thermal cavity and to a straightforward extension to accommodate the nozzle on the engine. The model gives, independently of both polarization and frequency, the formula  $\sigma = 2AF(\theta_i)F(\theta_s)\cos\theta_i\cos\theta_s$  for the narrowband bistatic RCS of the rocket-engine's extended signature, where  $\theta_i$  and  $\theta_s$  are, respectively, the angles between the engine axis and the lines of sight to the transmitting and receiving radars,  $A$  is the area of the nozzle throat, and  $F(\theta)$  is the nozzle gain factor. For a cavity with no nozzle,  $F(\theta) = 1$ .

The concept also produces a somewhat longer formula defining the wideband extended radar signature. It predicts, independently of incidence or scattering angles, polarization or frequency, a decay rate of  $2.17/L^*$  dB/m. ( $L^*$  is the *characteristic chamber length* defined in rocket engineering as the ratio of the chamber volume to the throat area.)

A second component of the scattered energy, the nonextended return, is the energy reflected by the nozzle without entering the combustion chamber. Added noncoherently to the energy disgorged by the combustion chamber, it gives the total signature.

The report presents the derivation of these formulas and then, by way of illustration, applies the model to a hypothetical rocket engine. It also includes predictions of the decay rates for a number of rocket engines, both foreign and domestic. Remarkably, the decay rates of six different high-thrust rocket engines all lie within a narrow 2-to-1 range, whereas their thrusts cover a 180-to-1 range.

The energy capture and release processes of the cavity are so simple to model that the overall model accuracy would seem to depend wholly on the assumption that the cavity energy is well mixed—a reasonably safe assumption for a rocket engine, as well as for other highly cluttered cavities. However, the report includes no comparison with measured data.

**This page intentionally left blank.**

## **ACKNOWLEDGMENTS**

I would like to acknowledge the encouragement and technical stimulation I received during this work from Douglas Koltenuk, Ryan Suess, and Allison Duncan.

**This page intentionally left blank.**



## TABLE OF CONTENTS

Abstract	iii
Acknowledgments	v
List of Illustrations	ix
1. CAVITY SIGNATURE: A THERMAL MODEL	1
1.1 Introduction	1
1.2 Basic Thermal Cavity	2
1.3 Nozzle Gain Factor	5
1.4 On-Axis Gain Factor for a Conical Nozzle	7
1.5 Discussion	8
1.6 Conclusions	10
APPENDIX	11
A.1 Basic Well-Mixed Thermal Cavity	11
A.2 Wideband Signature	11
A.3 Nozzle Gain-Factor Reciprocity	13
A.4 RCS Lobe-Width Estimate	13
A.5 On-Axis Gain Factor for a Conical Nozzle	14
A.6 Ray-Trace MATLAB Function	16

**This page intentionally left blank.**

## LIST OF ILLUSTRATIONS

Figure No.		Page
1	The basic cavity, showing the aperture, the single incidence direction, and the energy discharging along multiple scattering directions.	2
2	The wideband on-axis backscattered cavity signature for the basic well-mixed thermal cavity. The unrealistic abrupt start of the original formula is suppressed in the modified formula. The $y$ -axis units are square meters of radar cross section per meter of range, expressed in dB. (The effective cavity radius is the radius of a sphere having the same volume as the cavity.)	4
3	Four images showing ray paths through a plausible bell-shaped nozzle. The upper two show rays that penetrate the throat; the lower two show rays that do not. (The last one, lower right, shows a “whispering gallery” ray path, highly atypical.)	6
4	Gain factors for bell-shaped and conical nozzles. (The annotations are the coefficients of the polynomials defining the nozzle shapes.)	6
5	The nozzle shapes, together with their defining polynomial coefficients, used for generating the ray-trace images of Figure 3 and the nozzle gain-factor curves of Figure 4.	7
6	The on-axis gain factor for a “long” conical nozzle. The total on-axis RCS enhancement due to the nozzle is twice this. For a conical nozzle of arbitrary length, the on-axis gain factor is the lesser of the long-nozzle gain factor and the mouth-to-throat area ratio.	8
7	The extended-return decay rates of various liquid-fueled rocket engines, domestic and foreign, inferred from their characteristic chamber lengths.	9
8	The energy captured by the combustion chamber is the noncoherent integral over the hemispherical surface $C$ of the energy flux crossing it.	13

- 9 Throat penetration of a conical nozzle for axial incidence. All rays within the radius  $b'$  penetrate the nozzle throat. The direct rays (blue) lie within the central circle of radius  $a$ ; the single-reflection rays (red) lie outside that circle in the annulus of upper radius  $b'$ . If the cone half angle is more than  $22.5^\circ$ , only those two ray types can penetrate because the second reflection sends any ray obliquely back toward the nozzle mouth. 15
- 10 If the nozzle cone half angle is less than  $22.5^\circ$ , double-reflection rays can also penetrate the throat. These rays (green) lie in a second annulus lying outside the one occupied by the single-reflection rays (red). After the second reflection, they are still heading, obliquely, toward the nozzle throat. Triple-reflection rays achieve throat penetration only for cone half angles smaller than  $15^\circ$ . 16

# 1. CAVITY SIGNATURE: A THERMAL MODEL

## 1.1 INTRODUCTION

Cavities that generate long delayed radar returns present a difficult problem for radar signature modeling. Physically such cavities are either complicated (the end of a separated attitude control module with a crowded interior, for example) or they have the combination of a small aperture and a large volume (the combustion chamber of a liquid-fuel rocket or the burned-out case of a solid-fuel rocket). The long delay derives, in the first case, from the multiple scattering from objects within the cavity, and in the second, from the slow leakage imposed by the small aperture. Modeling such cavities electromagnetically, therefore, is simultaneously more important than modeling simple cavities but also more difficult.

A recent review by Anastassiou<sup>1</sup> of the various direct approaches to modeling cavities concludes that they all fail when the complexity of the cavity reaches a certain level. He describes exact methods using differential equations and integral equations, modal techniques, finite element methods, and the high-frequency, spectral, and ray-tracing methods. Unfortunately, the level of complexity at which they fail is still short of the levels reached by cavities of practical interest.

The thermodynamic model turns away from all these direct approaches. It approaches the problem from the other direction, by taking the complexity and slow leakage to their limits. Specifically, it introduces the concept of a well-mixed thermal cavity within which the captured radar energy is distributed uniformly in space, in direction of flow, and in polarization. It also assumes that the cavity is lossless. And, finally, it assumes that all dimensions of the cavity are large compared to a wavelength.

The consequences of these assumptions are simple formulas for the cavity's radar signature, narrowband and wideband. They apply to the basic well-mixed cavity for which the plane of the cavity aperture has full hemispheric exposure. The formulas depend only on the aperture area, the cavity volume, and the aspect angles, incident and scattering.

A rocket nozzle modifies the simple model. It shields the aperture (the nozzle throat) from the incoming radar energy at large aspect angles and increases its effective energy-collecting area at small aspect angles. It has the reciprocal effect on the energy discharge from the cavity, in that it narrows and intensifies its distribution. In fact, as will be demonstrated, the same numerical function of aspect, called here the nozzle gain factor, modifies both the energy collection and energy discharge.

An example, applying the model to a fictitious rocket engine with a bell-shaped nozzle, shows how large the magnifying effect of the nozzle can be. With the unexceptional dimensions of a 20° cone half

---

<sup>1</sup> H. T. Anastassiou, "A Review of Electromagnetic Scattering Analysis for Inlets, Cavities, and Open Duets," IEEE Antennas and Propagation Magazine, Vol. 45, No. 6, pp. 27-40 (Dec. 2003).

angle and a 9:1 area ratio of the mouth to the throat, the nozzle increases the on-axis backscattering RCS of the combustion chamber by some 18 dB.

## 1.2 BASIC THERMAL CAVITY

Figure 1 shows the generic basic cavity of volume  $V$  with a plane aperture of area  $A$ . If the incident energy flux density (Joules/m<sup>2</sup>) is  $W_i$ , and the aperture dimensions are large compared with a wavelength, then the total energy passing through the aperture into the cavity is simply  $W_i A \cos \theta_i$ . ( $\theta_i$  is the angle between the transmitting radar's line of sight and the aperture-plane normal.) If the cavity is lossless, all of this energy leaks back out again, its rate of leakage determined by the internal energy density and the aperture area, taking account of all the different directions with which it approaches the aperture. Section A.1 does the algebra, leading to the following simple formula, independent of polarization and frequency, for the narrowband bistatic RCS of the cavity:

$$\sigma = 2A \cos \theta_i \cos \theta_s,$$

where  $\theta_s$  is the angle between the receiving radar's line of sight and the aperture-plane normal.

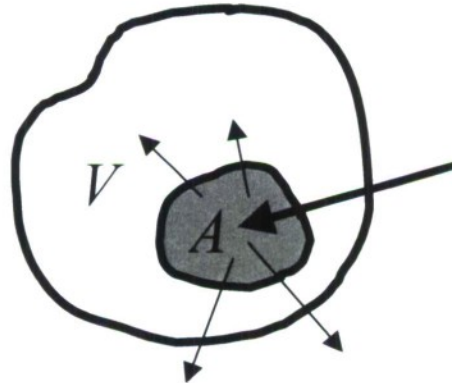


*Figure 1. The basic cavity, showing the aperture, the single incidence direction, and the energy discharging along multiple scattering directions.*

The frequency independence is based on the assumption that all dimensions of the cavity and the aperture are large compared with a wavelength. The smallest dimension, and therefore the limiting dimension, is likely to be that of the aperture. If it is not large, in wavelengths, then its effective area would be different from its actual area. And if it is below cut-off for electromagnetic wave transmission, no energy would enter the combustion chamber, and there would be no extended return at all. Fortunately,

since the cut-off radius is given<sup>2</sup> very closely by  $ka=1.8$  ( $k$  is the wave number and  $a$  the throat radius), at 10 GHz (X-band) the cut-off diameter  $2a$  is 1.7 cm. This is small compared to the throat diameter of large rocket motors, so for the higher-frequency radars we can expect the “large aperture” assumption usually to be satisfied. Moreover, the cut-off is very abrupt<sup>3</sup>. Above cut-off, the transmission is essentially perfect; below cut-off, there is none.

The wideband radar return from the cavity exhibits an extended return stretching out down-range of the cavity aperture. The measured length of the return is controlled by its decay rate, and that, in turn, is determined by the rate of leakage out through the aperture of the energy initially captured by the cavity. Section A.2, starting from the assumption that the incident radar energy instantaneously fills the cavity with a well-mixed thermal radiation field, derives this rate of leakage and then, by balancing the input and output energies, obtains the following explicit formula, plotted in Figure 2, for the wideband signature of the cavity’s extended return:

$$\Delta\sigma = \frac{\Delta r A^2 \cos\theta_i \cos\theta_s}{V} \exp(-Ar/2V).$$

Here,  $V$  is the cavity volume,  $A$  is the aperture area,  $\theta_i$  and  $\theta_s$  are, respectively, the angles between the aperture-plane normal and the radar lines of sight, transmitting and receiving,  $\Delta r$  is the radar’s range resolution, and  $r$  is the down-range distance from the cavity aperture. The ratio  $V/A$ , which occurs twice in this formula, is the quantity defined by Sutton and Biblarz<sup>4</sup> in their treatise on rocket propulsion as the *characteristic chamber length*  $L^*$  of the cavity.

In Figure 2, the line plot (labeled “original formula”) of this expression is normalized by  $\Delta r$ , applies to on-axis backscattering, and uses the unexceptional values 0.2 m for the equivalent radius of the cavity and 0.1 m for the aperture radius. Its unrealistic abrupt start is the result of the assumption that the well-mixed energy in the cavity is established instantaneously. The figure also shows a second line plot that includes a proposed correction for this problem.

The correction takes account of the fact that, initially, the bulk of the energy in the cavity is moving internally away from the aperture, and so little is flowing back out. This has the effect of delaying the apparent range at which the peak of the cavity return occurs. The rationale for the form of the adjustment is that if the cavity is the interior of a simple wide-open tin can, the range delay, for normal incidence, is simply the depth of the can. This depth is also equal to the volume of the can  $V$  divided by the area  $A$  of the aperture. That is, the depth is the characteristic chamber length  $L^*$ . This suggests that the formulas above for  $\Delta\sigma$  should be multiplied by the factor  $1-\exp(-r/L^*)$ , which rises from zero at  $r=0$  and approaches one for large  $r$ . This changes the formula for the distributed RCS of the cavity to

---

<sup>2</sup> A. Roberts, “Electromagnetic Theory of Diffraction by a Circular Aperture in a Thick, Perfectly Conducting Screen,” *J. Opt. Soc. Am.*, Vol. 4, No. 10, Oct. 1987.

<sup>3</sup> *Ibid.*

<sup>4</sup> G. P. Sutton and O. Biblarz, *Rocket Propulsion Elements*, John Wiley & Sons, New York, 2001.

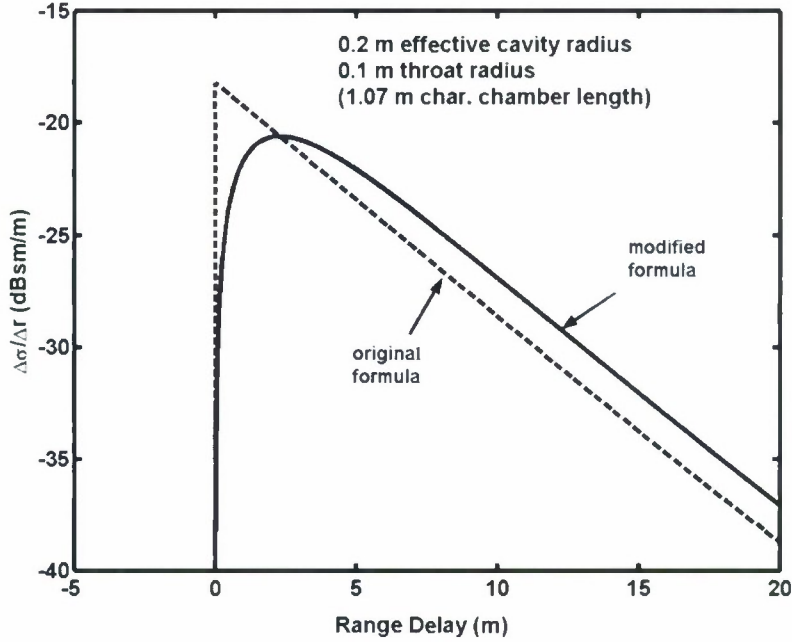


Figure 2. The wideband on-axis backscattered cavity signature for the basic well-mixed thermal cavity. The unrealistic abrupt start of the original formula is suppressed in the modified formula. The y-axis units are square meters of radar cross section per meter of range, expressed in dB. (The effective cavity radius is the radius of a sphere having the same volume as the cavity.)

$$\Delta\sigma = \frac{3\Delta r}{2L^*} A \cos\theta_i \cos\theta_s [1 - \exp(-r/L^*)] \exp(-r/2L^*),$$

in which now every occurrence of the ratio  $V/A$  has been replaced by  $L^*$ . The factor  $3/2$  ensures that the narrowband RCS remains at  $\sigma = 2A \cos\theta_i \cos\theta_s$ .

The asymptotic decay rate of the extended return in dB/m is given by the coefficient of  $r$  in the expression  $10\log_{10} \Delta\sigma$ ; it is  $(5/L^*) \log_{10} e$  or, equivalently,  $2.17/L^*$  dB/m. For the cavity and aperture dimensions used in Figure 2, the rate is 2.03 dB/m.

Another potentially significant adjustment to the formulas accommodates the more general situation in which the cavity is not lossless. Specifically, the additional exponential factor  $\exp(-t/\tau)$  is appended to the wideband formulas above, where  $\tau$  is the energy-decay time constant the cavity would have if closed. That is, the exponential factor  $\exp(-r/2L^*)$  is replaced by  $\exp(-r/2L^* - 2r/c\tau)$ , where  $c$  is the speed of light, and the equivalence relationship between time and range has also been applied. The corresponding adjustment to the narrowband formula is to multiply the lossless RCS by the factor  $(1 + 4L^*/c\tau)^{-1}$ .



### 1.3 NOZZLE GAIN FACTOR

A gain factor  $F_i(\theta_i)$  applied to the formula for the RCS of the basic cavity defines the way the nozzle of the rocket engine reshapes the energy-gathering pattern of the basic cavity aperture. A second gain factor  $F_s(\theta_s)$  defines the reshaping of its energy discharge. Section A.3 shows that, by reciprocity, these factors are identical—the subscripts  $i$  and  $s$  can be dropped. The narrowband and wideband bistatic RCS formulas for the basic thermal cavity thus become

$$\sigma = 2AF(\theta_i)F(\theta_s)\cos\theta_i\cos\theta_s$$

and

$$\Delta\sigma = \frac{3\Delta r}{2L^*}AF(\theta_i)F(\theta_s)\cos\theta_i\cos\theta_s(1 - \exp(-r/L^*))\exp(-r/2L^*) ,$$

respectively, when applied to the rocket engine.

Ray tracing can be used to evaluate the gain factor by counting how many more rays, of a uniform parallel flux of incident rays, pass through the aperture with the nozzle present. It involves tracing the ray reflections off the nozzle walls. Section A.5 illustrates the process for a conical nozzle. Section A.6 is the MATLAB function for evaluating the gain factor of a nozzle shape defined by an arbitrary polynomial.

Figure 3 shows the result of applying this MATLAB function to tracing four different rays interacting with a plausible bell-shaped nozzle. The rays in the upper two images penetrate the throat directly or after two reflections; those in the lower two reflect back out without penetrating the throat. (The trajectory of the highly atypical ray in the lower right image propels it along a “whispering gallery” path, undergoing multiple reflections as it moves around the inside wall.)

Two gain factor curves computed by the function, one for the bell-shaped nozzle and one for a similar conical nozzle, are presented in Figure 4. They show that a nozzle can have a substantial one-way on-axis gain—in this case nearly 10 dB. The total nozzle gain is twice this. The nozzle achieves this gain by narrowing the angular field both from which energy is gathered and to which it is discharged. These two gain-factor curves make the important point that the difference between the gain factors of a bell-shaped nozzle and of its conical nozzle approximation can be small enough that the latter will often be accurate enough.

Figure 5 shows the nozzle shapes themselves. The area ratio, mouth to throat, of both nozzles is 9, and the cone half angle of the conical nozzle is 20°.

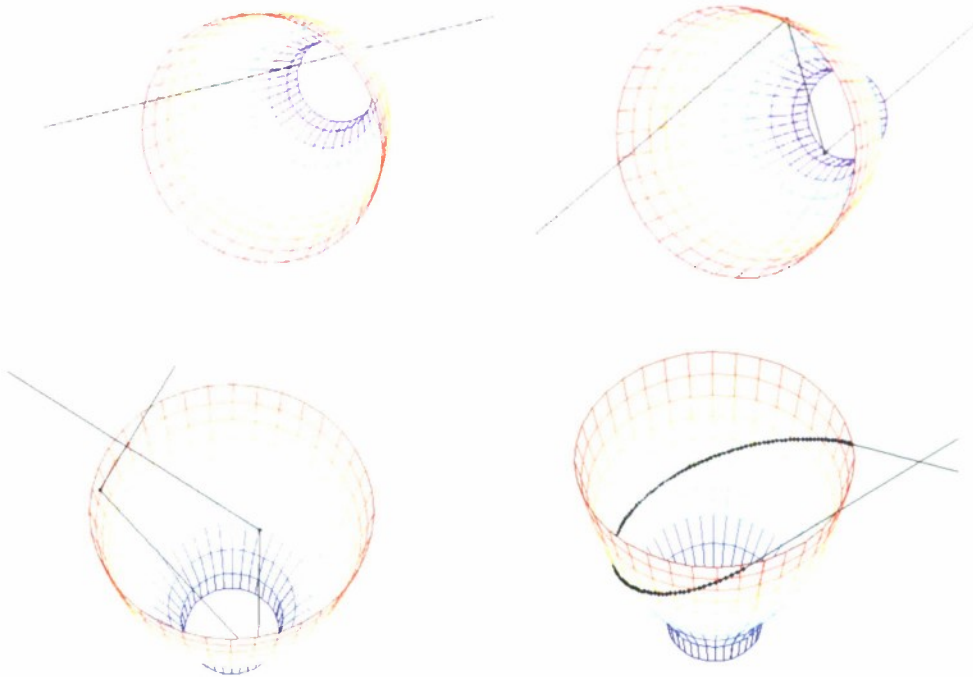


Figure 3. Ray paths through a plausible bell-shaped nozzle. The upper two show rays that penetrate the throat; the lower two show rays that do not. (The last one, lower right, shows a "whispering gallery" ray path, highly atypical.)

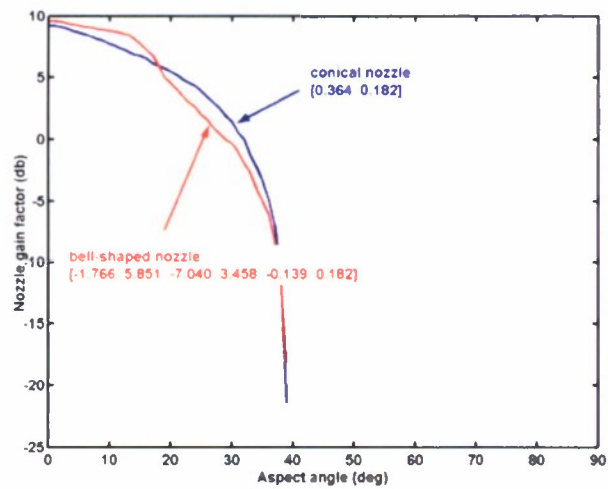


Figure 4. Gain factors for bell-shaped and conical nozzles. (The annotations are the coefficients, in MATLAB format, of the polynomials defining the nozzle shapes.)

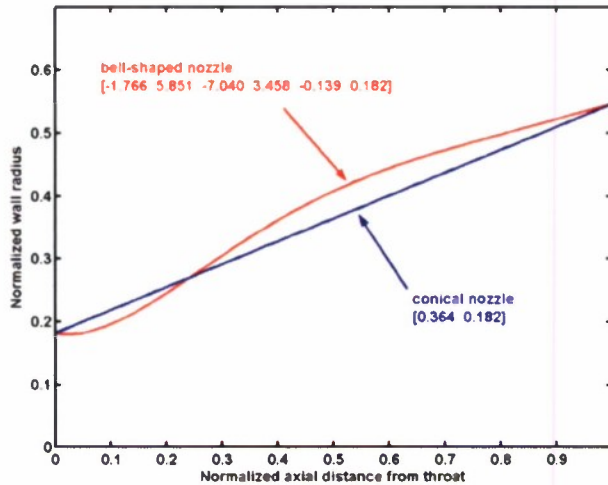


Figure 5. The nozzle shapes, together with their defining polynomial coefficients, used for generating the ray-trace images of Figure 3 and the nozzle gain-factor curves of Figure 4.

A useful measure of the gain factor curve is its angular half width  $\theta_w$ . It indicates the extent to which the nozzle narrows the view of the cavity, and it is readily estimated from the on-axis value of the gain factor. Section A.4, relying on the principle of energy conservation, demonstrates that the relationship is:

$$\theta_w = \arcsin(F^{-1/2}(0)).$$

But the gain factor of the actual nozzle can be evaluated with reasonable accuracy by considering its conical nozzle approximation. In particular, as the next section describes, the on-axis gain factor of a conical nozzle can be expressed in simple closed form. That provides a method for evaluating  $\theta_w$  without any numerical ray tracing.

For the case represented by the bell-shaped nozzle of Figure 4, this half width works out to be  $19.5^\circ$ , which corresponds to a point on the gain-factor curve 4.2 dB below its peak value. For the backscattering RCS, which involves the square of the gain factor as well as the square of  $\cos\theta$ , this point is 9.0 dB below the peak.

#### 1.4 ON-AXIS GAIN FACTOR FOR A CONICAL NOZZLE

The situation is particularly simple for a “short” purely conical nozzle with a cone half angle of less than  $45^\circ$ . At axial incidence, every ray incident within the nozzle mouth penetrates the throat and so  $F(0) = b^2/a^2$ , where  $a$  and  $b$  are, respectively, the throat and mouth radii. But if the nozzle is “long,” rays outside a certain radius get reflected back out of the nozzle and so do not penetrate the throat. The

effective energy-collection radius  $b'$  of the nozzle is then less than  $b$ , and  $F(0) = b'^2/a^2$ . In general, therefore,

$$F(0) = \min^2(b, b')/a^2.$$

Section A.5 shows that for the “long” nozzle with a half-angle  $\gamma$  between  $22.5^\circ$  and  $45^\circ$ ,  $b'/a = 4\cos^2\gamma - 1$ , and if  $\gamma$  lies between  $15^\circ$  and  $22.5^\circ$ ,  $b'/a = 16\cos^4\gamma - 12\cos^2\gamma + 1$ . Extending this process to even smaller cone half angles produces the plot in Figure 6.

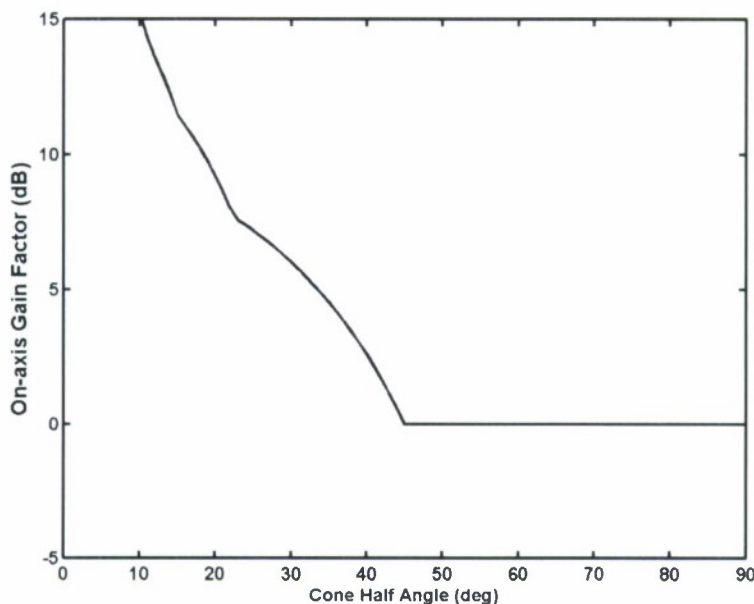


Figure 6. The on-axis gain factor for a “long” conical nozzle. The total on-axis RCS enhancement due to the nozzle is twice this. For a conical nozzle of arbitrary length, the on-axis gain factor is the lesser of the long-nozzle gain factor and the mouth-to-throat area ratio.

The graph shows that the nozzle can magnify the axial backscattering RCS of the combustion chamber by a large factor—some 18 dB in the case of a  $20^\circ$  cone half angle, if the radius ratio, mouth to throat, of the nozzle is no smaller than 7.94. (The RCS enhancement is, in dB, twice the gain factor.)

## 1.5 DISCUSSION

The ideal thermal model described above is limited. It cannot model simple cavities. For example, the narrowband RCS of a simple can-shaped cavity at normal incidence is about  $4\pi A^2/\lambda^2$  (the RCS of its base), whereas the corresponding thermal RCS is  $2A$ . At X-band, if the diameter is 1 m, these formulas imply the very different RCS values of 45.4 and 2.0 dBsm, respectively. The high number is not

significantly reduced if we include a small internal scatterer—much more complexity is necessary before the ideal thermal model becomes adequate.

It should also be noted that the cavity need not be complex to generate an extended return. Dumanian *et al.*<sup>5</sup> show a simple cylindrical cavity with an extended return stretching out behind the target more than fifteen times its physical depth, if the aspect angle is large. And they show that the extended return is not present at smaller aspect angles—very nonthermal behavior. Even though the energy within the cavity undergoes multiple bounces, the simple geometry of the cavity ensures that the bounces are very ordered. The energy is not well mixed.

On the other hand, if it is true that the energy is well mixed, then all that follows in producing the RCS formulas would seem to be logically necessary. Clearly wanting here are comparisons of the theory with some measured cavity-return data, but that must for the moment be handled in another context.

However, some testable predictions of the decay rate can be made from the values of  $L^*$  published for various real liquid-fueled rocket engines, domestic and foreign, by Sutton and Biblarz<sup>6</sup>. They are displayed in the graph in Figure 7.

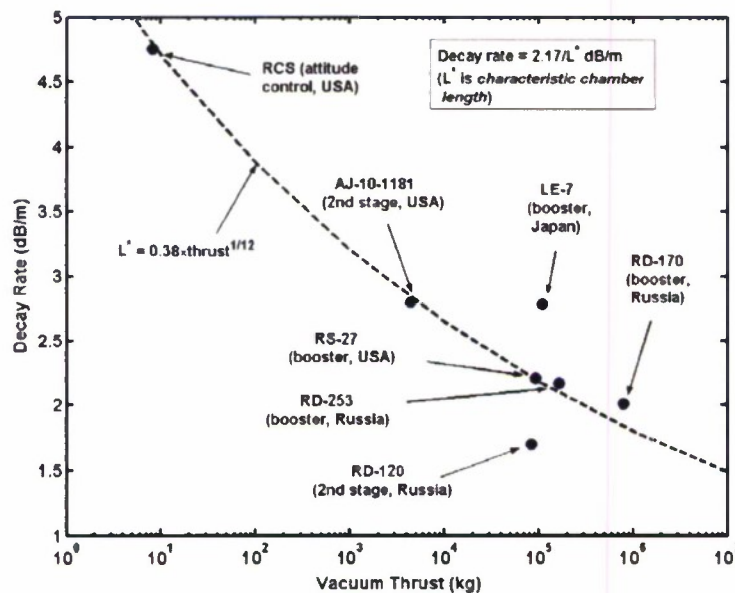


Figure 7. The extended-return decay rates of various liquid-fueled rocket engines, domestic and foreign, inferred from their characteristic chamber lengths.

<sup>5</sup> A. J. Dumanian, E. C. Burt, and B. A. Kemp, "A Component Model Approach for the RCS Validation of an Electrically Large Open-Ended Cavity" (to be published).

<sup>6</sup> G. P. Sutton and C. Biblarz, *op. cit.*, p. 272, 392.

A remarkable feature of these numbers is the relatively narrow range over which the extended-return decay rates of the high-thrust engines lie. These six engines, the largest of which has a thrust more than 180 times that of the smallest, differ in their predicted decay rates by a ratio no more than 1.64. How well these theoretical decay rates agree with the actual ones is yet to be determined.

A power-law curve with the engine's vacuum thrust as the independent variable is shown fitted to the plotted points. If nothing else, it provides a framework for the numbers.

## **1.6 CONCLUSIONS**

The well-mixed cavity model produces simple formulas for the extended radar signatures of liquid-fueled rocket engines and highly cluttered cavities. The energy capture and energy release processes of the cavity are so simple to model that the overall model accuracy depends wholly on the assumption that the cavity energy is well mixed—a seemingly safe assumption for these cavities. However, this report includes no comparison with measured data.

## APPENDIX

### A.1 BASIC WELL-MIXED THERMAL CAVITY

The energy  $E$  captured by the basic cavity is given by  $E = W_i A \cos \theta_i$ , where  $W_i$  is the incident energy flux density,  $A$  is the area of the cavity's aperture and  $\theta_i$  is the incidence angle (the angle between the line of sight to the transmitting radar and the normal to the plane of the aperture).

The perfect mixing assumption for the energy within the cavity implies that the energy within is uniformly distributed in its direction of propagation. That in turn implies that the reradiated energy flux density  $W_s$  in any direction is proportional to the projected area of the aperture in that direction. In other words, it is reradiated with a  $\cos \theta_s$  dependence on the scattering angle  $\theta_s$  (the angle between the line of sight to the receiving radar and the normal to the plane of the aperture), namely  $W_s = \alpha \cos \theta_s$ , with  $\alpha$  to be determined.

The total energy reradiated, for a lossless cavity, can be equated to the energy captured. That is, the reradiated energy flux density  $W_s$  must satisfy the equation  $E = R^2 \int W_s d\Omega_s$ . Carrying out this integral over the hemisphere, with  $W_s$  represented as  $\alpha \cos \theta_s$ , allows  $\alpha$  to be evaluated, and  $W_s$  to be expressed as  $W_s = W_i A \cos \theta_i \cos \theta_s / \pi R^2$ . This, together with the definition  $W_s = W_i \sigma / (4\pi R^2)$  for the radar cross section, yields the required expression for the bistatic narrowband *total* radar cross section of the basic well-mixed thermal cavity:  $\sigma = 4A \cos \theta_i \cos \theta_s$ .

Important to note here is the fact that this expression represents the total energy scattered by the cavity. According to the perfect mixing assumption, this must be divided equally, statistically, between whichever two orthogonal polarizations one chooses to define. The formula representing the true *measured* narrowband cross section therefore, evaluated at any polarization, is just half this, namely

$$\sigma = 2A \cos \theta_i \cos \theta_s .$$

### A.2 WIDEBAND SIGNATURE

Since the cavity is assumed to be lossless, the rate of decay of the energy in the cavity is equal to the total power flux back out through the aperture. This can be evaluated from the total energy  $E$  currently in the cavity using the well-mixed cavity assumption.

Specifically, the directional energy density in the cavity is  $E / 4\pi V$  Joules/m<sup>3</sup>/steradian, where  $V$  is the cavity volume, so the directional power flux density is  $Ec / 4\pi V$  watts/m<sup>2</sup>/steradian, where  $c$  is the speed of light, and the directional power flux thorough the aperture is  $EcA \cos \theta / 4\pi V$  watts/steradian, where  $A$  is the aperture area and  $\theta$  is the angle between the propagation direction and the aperture-plane

normal. The total power flux through the aperture is the integral of this over the external hemisphere, that is,  $(cA/4V)E$  watts. This is the negative of the rate of change of the total energy in the cavity, implying that the total energy in the cavity decays according to the law

$$E = W_i A \cos \theta_i \exp(-cAt/4V),$$

where the factor combination  $W_i A \cos \theta_i$  represents the initial energy captured by the cavity.

The result of substituting this expression for  $E$  into the formula  $E c A \cos \theta_s / 4\pi V$  from the previous paragraph for the directional power flux through the aperture in the direction of the receiving radar converts it into

$$\frac{cA^2 W_i \cos \theta_i \cos \theta_s}{4\pi V} \exp(-cAt/4V).$$

Its units are watts/steradian.

Multiplying this same expression by the small time increment  $\Delta t$  (the range resolution  $\Delta r$  expressed in units of time) gives the combined incremental radar-directed energy flux (Joules/steradian) of both polarizations, which, from the definition of radar cross section, is also equal to twice the incremental radar cross section  $\Delta \sigma$  measured in any one polarization times the incident energy flux  $W_i$  (Joules/m<sup>2</sup>) divided by  $4\pi$ . Solving this equation for  $\Delta \sigma$ , and observing the equivalence of  $ct$  with  $2r$ , finally yields the following expression for the bistatic incremental wideband RCS of the basic well-mixed cavity:

$$\Delta \sigma = \frac{\Delta r A^2 \cos \theta_i \cos \theta_s}{V} \exp(-Ar/2V).$$

The narrowband RCS is the range integral of  $\Delta \sigma / \Delta r$ , namely  $\sigma = 2A \cos \theta_i \cos \theta_s$ , which agrees, as it should, with the direct derivation of the previous section.

Here,  $V$  is the cavity volume,  $A$  is the aperture area,  $\theta_i$  and  $\theta_s$  are, respectively, the angles between the aperture-plane normal and the radar lines of sight, transmitting and receiving, and  $\Delta r$  is the radar's range resolution.

The asymptotic decay rate of the extended return in dB/m is given by the coefficient of  $r$  in the expression  $10 \log_{10} \Delta \sigma$ ; it is  $(5A/V) \log_{10} e$  or, equivalently,  $2.17 A/V$  dB/m.



### A.3 NOZZLE GAIN-FACTOR RECIPROCITY

The reciprocity theorem implies that the nozzle gain factor shaping a combustion chamber's energy capture is the same function of aspect as the nozzle gain factor shaping the combustion chamber's energy discharge.

For proof of this statement, it is useful to imagine the nozzle alone, unattached to its combustion chamber. Then, the radar-pulse energy captured by the cavity is the noncoherent integral over the hemispherical surface  $C$  of the energy penetrating the nozzle throat (see Figure 8). In the other direction, the total energy radiating from the mouth of the cavity back in the direction of the radar is the noncoherent integral over the hemispherical surface  $C$  of the energy radiated in the direction of the radar by each one of a uniform distribution of identical emitters. (The emitters are identical and uniformly distributed over  $C$  because, according to the assumptions of the thermal cavity model, the radiation field inside the cavity is uniformly distributed in direction.)

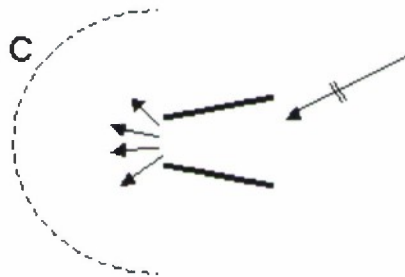


Figure 8. The energy captured by the combustion chamber is the noncoherent integral over the hemispherical surface  $C$  of the energy flux crossing it.

The reciprocity theorem equates, on the one hand, the field at each point on surface  $C$  due to the radar, and, on the other, the field at the radar due to each point emitter on surface  $C$ . This equality extends, therefore, to the two integrals.

### A.4 RCS LOBE-WIDTH ESTIMATE

The expression  $F(\theta)\cos\theta$  involving the nozzle gain factor fully describes the directional properties of the engine's radar signature. But a rough indication of the main-lobe half width  $\theta_{1/2}$  of the RCS can be derived that depends only on the on-axis value  $F(0)$ . The derivation depends on the statement  $E = 2R^2 \int W_s d\Omega_s$  of the conservation of energy, equating the total energy captured by the combustion chamber to the total energy reradiated. Here  $2W_s$  is the total reradiated energy flux density

( $W_s$  in each polarization) as a function of solid angle  $\Omega_s$  and the integration is carried out over the hemispherical surface of (large) radius  $R$  across which the energy passes.

The application to this conservation statement of the three identities  $E = W_i AF(\theta_i)\cos\theta_i$  (for the total energy captured by the combustion chamber),  $W_s = W_i\sigma/(4\pi R^2)$  (for the definition of radar cross section), and  $\sigma = 2AF(\theta_i)F(\theta_s)\cos\theta_i\cos\theta_s$  (for the radar cross section of the combined combustion chamber and nozzle for each polarization), reduces it to  $1 = \pi^{-1} \int F(\theta_s)\cos\theta_s d\Omega_s$ . ( $A$  is the nozzle throat area and  $W_i$  the incident energy flux density.) And since  $d\Omega_s = \sin\theta_s d\theta_s d\phi_s$ , this can be rewritten

$$1 = \int_0^{\pi/2} F(\theta_s)\sin 2\theta_s d\theta_s = F(0) \int_0^{\theta_w} \sin 2\theta_s d\theta_s,$$

where  $\theta_w$  is the main-lobe half width. Evaluating the integral and then solving for  $\theta_w$  leads to the result

$$\theta_w = \arcsin(F^{-1/2}(0)).$$

## A.5 ON-AXIS GAIN FACTOR FOR A CONICAL NOZZLE

For a conical model of the nozzle, the simple ray geometry for axial incidence allows easy evaluation of the gain factor on-axis. If the cone half angle  $\gamma$  is greater than  $45^\circ$ , the nozzle gain factor at axial incidence is 1; in other words, at axial incidence no ray can penetrate the nozzle throat after reflection off the nozzle wall and so the nozzle has no effect. The only energy to penetrate the nozzle throat does so directly, just as it would were no nozzle present.

For cone half angles less than  $45^\circ$ , but no smaller than  $22.5^\circ$ , the only rays that penetrate the throat at axial incidence are those that pass either directly through the throat or through it after one reflection off the nozzle wall. The circular symmetry of the nozzle ensures that this additional collection area is a circle with a radius  $b'$  that is bigger than the radius  $a$  of the nozzle throat. Every incident ray that is within a radius  $b'$  of the nozzle axis penetrates the throat, either directly or after one reflection off the nozzle wall. Thus, the gain factor is simply the ratio of the two circle areas, specifically  $(b'/a)^2$ . This ray geometry is shown in Figure 9. However, if the nozzle is short enough, the radius of its energy collection circle will be just  $b$ , the radius of the nozzle mouth. Thus, in general, the gain factor will be  $\{\min(b',b)/a\}^2$ . Evaluating  $b'$  is a simple exercise in trigonometry. The final solution for the gain factor for axial incidence is then

$$F(0) = \min^2[4\cos^2(\gamma) - 1, b/a], \quad (22.5^\circ < \gamma < 45^\circ),$$

where  $b$  and  $a$  are the mouth and throat radii of the nozzle and  $\gamma$  is the cone half angle.

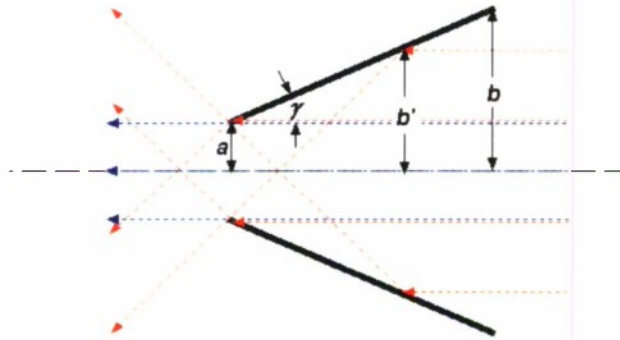


Figure 9. Throat penetration of a conical nozzle for axial incidence. All rays within the radius  $b'$  penetrate the nozzle throat. The direct rays (blue) lie within the central circle of radius  $a$ ; the single-reflection rays (red) lie outside that circle in the annulus of upper radius  $b'$ . If the cone half angle is more than  $22.5^\circ$ , only those two ray types can penetrate because the second reflection sends any ray obliquely back toward the nozzle mouth.

For smaller cone half angles, down to  $15^\circ$ , at axial incidence, some rays also penetrate the throat after two reflections off the nozzle wall, as shown in Figure 10. In this situation, following the same logic as for the one-reflection case, the gain factor for axial incidence is given by

$$F(0) = \min^2[16 \cos^4(\gamma) - 12 \cos^2(\gamma) + 1, b/a] \quad (15^\circ < \gamma < 22.5^\circ).$$

Since the total gain factor is the product of the collecting and discharge gain factors, and since these factors are equal, the total gain factor of the nozzle for backscattering at axial incidence is simply  $F^2(0)$ .

This analysis is readily extended to smaller cone half angles with their penetrating rays of even greater bounce count. The resulting gain factor is presented graphically in Figure 6 in the main text, in which the “long nozzle” assumption is made. That is, it is assumed that the nozzle mouth radius is larger than the geometric collecting radius determined by the formulas in  $\cos(\gamma)$ . The graph shows that the nozzle can magnify the axial backscattering RCS of the combustion chamber by a large factor—some 18 dB in the case of a  $20^\circ$  cone half angle, if the radius ratio, mouth to throat, of the nozzle is no smaller than 7.94.

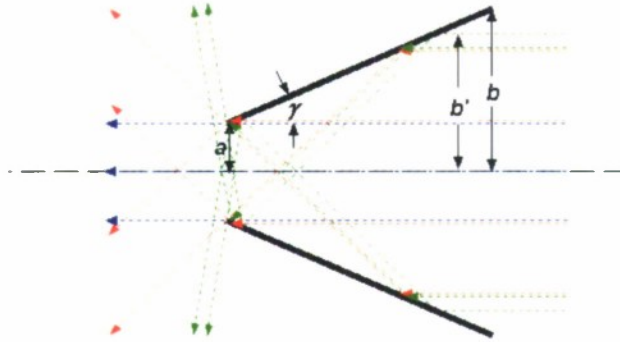


Figure 10. If the nozzle cone half angle is less than  $22.5^\circ$ , double-reflection rays can also penetrate the throat. These rays (green) lie in a second annulus lying outside the one occupied by the single-reflection rays (red). After the second reflection, they are still heading, obliquely, toward the nozzle throat. Triple-reflection rays achieve throat penetration only for cone half angles smaller than  $15^\circ$ .

#### A.6 RAY-TRACE MATLAB FUNCTION

The following MATLAB function uses ray tracing to evaluate the gain factor at a single angle of incidence  $\theta$  for a nozzle whose shape is specified by a polynomial defining the radius  $\rho$  of the inside surface of the nozzle wall as a function of the axial dimension  $z$ .

It traces the paths of a large number  $N$  of parallel rays uniformly distributed, statistically, over the nozzle mouth, scoring a one for each ray that eventually passes through the nozzle throat and a zero for each ray reflected back out of the nozzle mouth without ever passing through the throat. The total score  $N_t$  divided by  $N$  then represents the fraction of the total energy incident on the nozzle mouth that passes through the throat. Therefore, the nozzle gain factor, defined as the factor by which the energy passing through the throat with the nozzle present exceeds the energy passing through the throat with the nozzle absent, is computed as  $(b^2 / a^2)N_t / N$ , where  $a$  and  $b$  are, respectively, the radii of the nozzle throat and mouth.

The four images in Figure 3 show the paths of four rays computed using the ray-tracing feature of the MATLAB function, two of which penetrate the throat and two that do not. Two gain factor curves computed by the function, one for the bell-shaped nozzle and one for a conical-nozzle approximation to it, are presented in Figure 4.

```

function G=PolyNozzleGain(c,thdeg,N)

% G is the gain factor (not in dB) of the nozzle at the aspect angle thdeg.
% The radius rho of the nozzle as a function of the axial dimension z is defined
% by the polynomial c: rho = c(1)*z^M + ... +c(M) *z + c(M+1).
% The nozzle throat is at z = 0; the nozzle mouth is at z = 1.
% N rays are used, uniformly distributed (statistically) over the nozzle mouth.
% c=[-1.7663 5.8506 -7.0398 3.4583 -0.13876 0.18199]; % 9-to-1 bell nozzle
% c=[0.364 0.182]; % 9-to-1 cone nozzle

a=polyval(c,0);b=polyval(c,1);
G=0; n=0;
while n<N
    x=b*(2*rand-1);y=b*(2*rand-1);
    if x^2+y^2<=b^2
        n=n+1;
        G=G+PolyNozzleTrace(c,thdeg,x,y);
    end
end
G=G*b^2/N/a^2;

function K=PolyNozzleTrace(c,thdeg,x,y)

% checks to see whether a particular ray incident on the nozzle mouth
% penetrates throat
% c lists the polynomial coefficients for the nozzle contour: rho = c(1)*z^M + ... % +c(M) *z + c(M+1)
% thdeg is the aspect angle
% x,y are the coordinates of the point at which the incident ray
% crosses the plane of the nozzle's exit aperture
% K is 1 if the ray penetrates the throat and 0 if it does not

M=length(c)-1; th=thdeg*pi/180;
A=PolyBase(conv(c,c)); % the coefficient generator matrix
r1=[x y 1]; % the starting point of the ray in the plane of the nozzle mouth
p1=[-sin(th) 0 -cos(th)]; % the starting direction of the ray
for k=0:100
    r0=r1;p0=p1;
    Ls=roots([zeros(1,2*M-2) 1-p0(3).^2 2*r0(1:2)*p0(1:2)' r0(1:2)*r0(1:2)']-...
        (r0(3).^(0:2*M))*A.*(p0(3).^fliplr(0:2*M)));
    I=find(imag(Ls)==0);Lre=Ls(I); % discard the complex roots
    I=find(Lre>1e-6);Lpos=Lre(I); % discard all non positive definite values of L
    L=min(Lpos); % retain only the first encounter with the surface
end

```

```

if length(L)==0 & p0(3)<0, % no bounce point; ray passes directly through throat
    K=1;return,end
if length(L)==0 & p0(3)>=0 % no bounce point; ray is reflected back
    K=0;return,end
r1=r0+L*p0; % the bounce point
if r1(3)<0 % bounce point beyond throat; ray passes directly through
    K=1;return,end
if r1(3)>1 % bounce point before mouth; ray is reflected back
    K=0;return,end
t=polyval(polyder(c),r1(3)); % the surface slope at the bounce point
n1=[r1(1:2) -t*sqrt(r1(1:2)*r1(1:2))]; % the surface normal at the bounce point
n1=n1/sqrt(n1*n1'); % the unit surface normal
p1=p0-2*n1*(n1*p0'); % the pointing direction of the reflected ray
end
% the ray has exceeded 100 bounces, so it's counted as not passing through the throat
K=0;

```

```
function A=PolyBase(PM)
```

```

% A is the matrix determining the coefficients of the polynomial with argument x formed
% from the polynomial PM of degree M having as argument the first degree polynomial
% P1. Those coefficients are (P1(2).^(0:M))*A.*(P1(1).^fliplr(0:M));

```

```
M=length(PM)-1;
```

```
A=(ones(M+1,1)*[PM 0]);
```

```
A=triu(fliplr(pascal(M+1))).*reshape(A(1:(M+1)^2),M+1,M+1);
```

# REPORT DOCUMENTATION PAGE

*Form Approved*  
OMB No. 0704-0188

Public reporting burden for this collection of information is estimated to average 1 hour per response, including the time for reviewing instructions, searching existing data sources, gathering and maintaining the data needed, and completing and reviewing this collection of information. Send comments regarding this burden estimate or any other aspect of this collection of information, including suggestions for reducing this burden to Department of Defense, Washington Headquarters Services, Directorate for Information Operations and Reports (0704-0188), 1215 Jefferson Davis Highway, Suite 1204, Arlington, VA 22202-4302. Respondents should be aware that notwithstanding any other provision of law, no person shall be subject to any penalty for failing to comply with a collection of information if it does not display a currently valid OMB control number. **PLEASE DO NOT RETURN YOUR FORM TO THE ABOVE ADDRESS.**

<b>1. REPORT DATE</b> 18 December 2008			<b>2. REPORT TYPE</b> Technical Report		<b>3. DATES COVERED (From - To)</b>	
<b>4. TITLE AND SUBTITLE</b>  Extended Radar Return from a Rocket Engine: A Thermal Model					<b>5a. CONTRACT NUMBER</b> FA8721-05-C-0002	
					<b>5b. GRANT NUMBER</b>	
					<b>5c. PROGRAM ELEMENT NUMBER</b> 1057	
<b>6. AUTHOR(S)</b>  Michael L. Burrows					<b>5d. PROJECT NUMBER</b>	
					<b>5e. TASK NUMBER</b> 2	
					<b>5f. WORK UNIT NUMBER</b>	
<b>7. PERFORMING ORGANIZATION NAME(S) AND ADDRESS(ES)</b> AND ADDRESS(ES)  MIT Lincoln Laboratory 244 Wood Street Lexington, MA 02420-9108					<b>8. PERFORMING ORGANIZATION REPORT NUMBER</b>  TR-1123	
<b>9. SPONSORING / MONITORING AGENCY NAME(S) AND ADDRESS(ES)</b>  Missile Defense Agency 7100 Defense Pentagon Washington, DC 20301					<b>10. SPONSOR/MONITOR'S ACRONYM(S)</b>	
<b>11. SPONSOR/MONITOR'S REPORT NUMBER(S)</b> ESC-TR-2006-090					<b>12. DISTRIBUTION / AVAILABILITY STATEMENT</b>  Approved for public release; distribution is unlimited.	
<b>14. ABSTRACT</b> <p>Conventional modeling methods are inadequate for handling the extended radar return caused by the slow release of the radar energy captured by a deep cavity. The complexity overwhelms them.</p> <p>The length of the extended return implies that the captured energy undergoes a great many internal reflections before it reemerges, suggesting treating the captured energy as a well-mixed thermal radiation field.</p> <p>This suggestion leads to a simple scattering model for the well-mixed lossless thermal cavity and to a straightforward extension to accommodate an engine nozzle. The model gives, independently of polarization and frequency, the formula <math>\sigma = 2AF(\theta_t)F(\theta_r)\cos\theta_t\cos\theta_r</math> for the narrowband bistatic RCS of the rocket-engine's extended signature, where <math>\theta_t</math> and <math>\theta_r</math> are, respectively, the angles between the engine axis and the lines of sight to the transmitting and receiving radars, <math>A</math> is the area of the nozzle throat, and <math>F(\theta)</math> is the nozzle gain factor. For a cavity with no nozzle, <math>F(\theta) = 1</math>.</p> <p>The concept produces a somewhat longer formula defining the wideband extended radar signature. It predicts, independently of incidence or scattering angles, polarization or frequency, a decay rate of <math>2.17/L^*</math> dB/m. (<math>L^*</math> is the <i>characteristic chamber length</i> defined in rocket engineering literature as the ratio of the chamber volume to the throat area.)</p>						
<b>15. SUBJECT TERMS</b>						
<b>16. SECURITY CLASSIFICATION OF:</b>			<b>17. LIMITATION OF ABSTRACT</b>		<b>18. NUMBER OF PAGES</b>	<b>19a. NAME OF RESPONSIBLE PERSON</b>
<b>a. REPORT</b> Unclassified	<b>b. ABSTRACT</b> Unclassified	<b>c. THIS PAGE</b> Unclassified	Same as report		30	<b>19b. TELEPHONE NUMBER (include area code)</b>